

Article

Hydrological Properties of a Clay Loam Soil as Affected by Biochar Application in a Pot Experiment

Angela Libutti *, Matteo Francavilla and Massimo Monteleone

Department of Science of Agriculture, Food, Natural Resources and Engineering, University of Foggia, 71122 Foggia, Italy; matteo.francavilla@unifg.it (M.F.); massimo.monteleone@unifg.it (M.M.)

* Correspondence: angela.libutti@unifg.it; Tel.: +39-0881-589128

Abstract: Improving soil-water relations by amending soil with biochar might play a significant role in increasing water availability for agricultural crops as well as decreasing water loss through drainage or runoff. While the effects of biochar on the hydrological properties on coarse-textured soils are generally positive and well-documented in the literature, studies on biochar effects on fine-textured soils are rather scarce and even contradictory. Therefore, the aim of this paper was to investigate the impact of biochar on the bulk density, water retention curve (together with several water capacitive indicators) and water infiltration rate in a clay loam soil. A pot experiment was carried out under lab conditions in which biochar was mixed with soil at rates of 0 (B0 or control), 2, 4, 6, 8 and 10% dw (B2, B4, B6, B8 and B10, respectively). Water retention of soil–biochar mixtures at different matrix potentials was determined using a pressure plate apparatus. From these measurements, a series of capacitive indicators was derived and the fitting of the van Genuchten model was also performed. Water infiltration into soil–biochar mixtures was measured by means of a mini-disk infiltrometer and the obtained data were analyzed both directly and by fitting the Philip’s model. Biochar significantly affected the considered soil properties. As the biochar rate increased, the bulk density decreased and water retention increased (B6, B8 and B10 > B2, B4 and B0), while the infiltration rate decreased (B0 > B2, B4, B6, B8 and B10). Although the experiment was performed on sieved and repacked soil samples under lab conditions, the results confirmed that biochar has the potential to increase plant-available water, while possibly reducing drainage water in a clay loam soil by lowering the infiltration rate.

Citation: Libutti, A.; Francavilla, M.; Monteleone, M. Hydrological Properties of a Clay Loam Soil as Affected by Biochar Application in a Pot Experiment. *Agronomy* **2021**, *11*, 489. <https://doi.org/10.3390/agronomy11030489>

Academic Editors: Lukas Trakal and Elena Maestri

Received: 8 January 2021

Accepted: 2 March 2021

Published: 5 March 2021

Keywords: biochar; soil bulk density; soil hydrological properties; soil capacitive indicators; soil water retention; soil available water; soil water infiltration; mini disk infiltrometer; van Genuchten model; Philip’s infiltration model

Publisher’s Note: MDPI stays neutral with regard to jurisdictional claims in published maps and institutional affiliations.



Copyright: © 2021 by the authors. Licensee MDPI, Basel, Switzerland. This article is an open access article distributed under the terms and conditions of the Creative Commons Attribution (CC BY) license (<http://creativecommons.org/licenses/by/4.0/>).

1. Introduction

Over the last decade, the use of biochar as a soil organic amendment has attracted increasing interest for its environmental and agronomic benefits, which is well-documented in several reviews and meta-analyses [1–4]. Biochar is a carbon-rich (60–80% C) material that can be obtained from different feedstocks (forest wood, manure, sewage sludge, agriculture residues) under a high-temperature treatment (from 300 to 1200 °C) and in an oxygen-limited environment (pyrolysis or gasification) [5–7]. With regard to environmental sustainability, biochar, due to its long-term stability in soil, has been reported to have great climate mitigation potential [8] for its ability to sequester atmospheric CO₂ and reduce greenhouse gas (GHG) emission [9]. Concerning its agronomic implications, biochar has been shown to increase physical, chemical and microbiological soil fertility as well as reduce nutrient leaching and improve crop yield response [10–13]. In recent years, biochar application has also been suggested for controlling soil and water pollution by holding contaminants that are both inorganic (nitrogen, phosphorous, heavy

metals) and organic (pesticides, herbicides, antibiotics) [14]. These biochar properties are mainly due to its highly porous structure, large inner surface area, greater negative surface charge and charge density [15,16].

Experimental evidence suggest that the physical properties of biochar (porosity and surface area) could improve not only soil physical properties (e.g., porosity, bulk density and aggregate stability) but also hydrological properties, including water retention and hydraulic conductivity [2,17]. Increases in soil water retention following biochar addition have been extensively reported in the literature, under both controlled (laboratory, lysimeters and pots) and open-field conditions. Several authors observed the rise in water retention on coarse- and medium-coarse textured soils amended with both lower [18,19] and higher biochar doses ($>15 \text{ Mg ha}^{-1}$) [20,21]. Conversely, other authors reported no changes in water retention in fine-textured soils following biochar addition [22,23]. This clearly suggests that the biochar effect is largely dependent on soil type (texture and structure) and application rate. Moreover, it was reported that the effect of biochar on water retention is also linked to original feedstock and applied thermochemical conditions [23]. In this regard, an improvement of water retention was observed on coarse-textured soils after the application of two types of gasification biochar [19], while no effects were detected after applying biochar obtained from straw and pine wood at different pyrolysis temperatures [24]. A number of studies also report contrasting effects of biochar on saturated and unsaturated soil hydraulic conductivity (K_{sat} and K_{unsat} , respectively). Biochar sometimes increased, sometimes decreased K_{sat} , while limited results about the effects on K_{unsat} were reported. Similar to water retention, the biochar effect on hydraulic conductivity is dependent on soil texture [1]. Several studies [25,26] reported a K_{sat} decrease in sandy soil after biochar addition. Similar results were found by other authors [27] in coarse sand and fine sand soils, although they found a K_{sat} increase in clay loam soil. Likewise, K_{sat} increase was reported in poorly drained silty loam, silty clay and clay soil by several authors [16,28,29]. All these studies were conducted under controlled conditions (column, laboratory and greenhouse), but K_{sat} increase was also observed in field experiments on clay soils [30,31]. Soil hydraulic conductivity is also influenced by biochar type and application rate. Indeed, K_{unsat} increase was found after wood biochar addition to soil [25]; in laboratory experiments on clay soil, a significant K_{sat} increase was observed at higher biochar rates with no difference for K_{unsat} [32]. It was also reported that biochar hydrophobicity could induce water repellency and reduce hydraulic conductivity [33]. The hydrophobic nature of biochar decreases with increasing pyrolysis temperature [34], and biochar obtained at lower temperatures could be very water repellent due to alkyl groups on its surface [35].

If applying biochar to cultivated soil increases water retention, it could, in turn, increase plant-available water. This effect can be attributed to water retained in the pores within the biochar structure (intrapores) and those formed at the interface between biochar and soil particles or within small aggregates (interpores) [36]. Micropores can hold water strongly through capillary and adhesive forces, and mesopores contain water readily available to plants, while macropores are easily drained [1]. The increased micro- and meso-porosity due to biochar addition could explain why coarse-textured soils are more benefitted than fine-textured ones. Apart from soil porosity, also soil structure may play a relevant role [37]. In sandy loam, biochar promoted soil aggregation and aggregate stability due to the addition of organic carbon. Conversely, in clay soil, larger biochar doses strengthened repulsive forces between particles and monovalent cations, producing colloid dispersion and aggregate breakdown [37,38].

Moreover, biochar decreases hydraulic conductivity in sandy soils, thereby reducing the risk of nutrient leaching, whereas it increases hydraulic conductivity in fine-textured soils, thus enhancing water infiltration and limiting water runoff [1]. The mechanisms generally reported to explain these effects on conductivity in sandy soil are the filling or clogging of macropores by fine biochar particles and the increase in the number of micropores that bind water by strong capillary and adsorptive forces [27]; in fine-texture soil,

the mechanisms are the improvement of aggregation and aggregate stability by biochar [39]. However, some exceptions to this general scheme were also detected [40–43].

In a previous paper from our research team [13], we reported the results of biochar application to a loam-texture soil in a 2-year field experiment made of four consecutive crop-growing cycles. The applied biochar played an important role in reducing water drainage loss, thereby limiting nutrient leaching. However, a “threshold effect” was observed: when a lower biochar amount was applied, the increase in water retention prevailed over the increase in water conductivity, causing diminished drainage; conversely, when a higher biochar amount was added, the reverse effect occurred, and drainage was greater. This must be considered our starting study hypothesis that must be verified. We did not perform any direct measurements of hydraulic soil properties in that previous field experiment, and our supposed explanation cannot be demonstrated until a new field experiment is performed. Nevertheless, prior to performing this further field trial, we considered working out a pot experiment in order to shed some light on this specific issue. Therefore, strictly controlled lab conditions were applied to a fine-textured soil similar to the one previously used. We are aware that, compared to in situ soils, the use of sieved and repacked soil in pots can be of concern when studying soil physical properties. Indeed, soil structure, pore architecture and pore size distribution are deeply altered when sieved and repacked soil is used, and the consequent soil hydraulic properties can change dramatically. However, under these strictly controlled experimental conditions, more extensive and accurate measurements can be performed and the effects of different biochar addition rates can be better compared and discriminated.

The aim of the present study was to evaluate whether biochar application could affect soil hydraulic properties in a clay loam soil in pots under lab conditions. The effect of different rates of biochar addition on bulk density, water retention curve, together with a set of water-capacitive indicators and water infiltration rates, was analyzed. No attempts were made to extrapolate the obtained results to “in-field” soil conditions, but deeper insights into how biochar operates in a soil mixture at different addition rates can surely promote more focused research activities in the open field.

2. Materials and Methods

Figure 1 shows the sequential phases applied when performing our experiment: from soil and biomass sampling, through biochar production and preparing soil–biochar mixtures, to measurements and data interpretation.

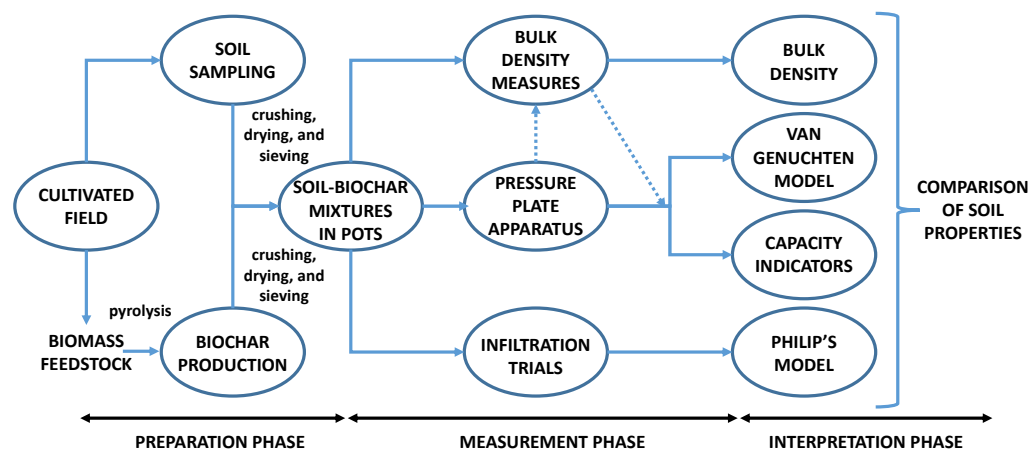


Figure 1. Flow chart summarizing the phases in which the experimental procedure adopted in this work is divided.

2.1. Soil and Biochar Preparation and Characterization

Soil samples were collected from the 0–0.20 m upper soil layer in Foggia, South Italy (latitude 41°27' N, longitude 15°32' E). The soil was oven dried at 105 °C until reaching a constant weight, after which it was crushed and passed through a 2 mm sieve. The particle size distribution was analyzed by the pipette-gravimetric method and the soil type was determined according to the USDA (United States Department of Agriculture) soil classification [44]. The pH was measured on a 1:2.5 (w/v) soil/water suspension with deionized water by a digital pH meter (GLP 22 pH-meter, Crison Instruments, Barcelona, Spain) and the electrical conductivity (EC) on saturated soil paste extract by a digital conductivity meter (GLP 31 EC-meter, Crison Instruments, Barcelona, Spain). Total nitrogen (total N) was determined by the Kjeldahl method [45] and the available phosphorus (P₂O₅) by extraction with sodium bicarbonate [46]. Organic carbon was determined by the dichromate oxidation method [47] and converted to organic matter (OM) by the conventional factor 1.724. The soil was of a clay loam texture, poor in nitrogen but rich in available phosphorus, with low organic-matter content, an alkaline pH and low electrical conductivity (Table 1).

Table 1. Main physicochemical characteristics of soil samples.

Characteristic	Value ¹
Clay (%)	37.09 ± 0.91
Silt (%)	36.23 ± 1.08
Sand (%)	26.68 ± 0.28
pH (-)	8.26 ± 0.06
² EC (dS m ⁻¹)	0.47 ± 0.01
P ₂ O ₅ (mg kg ⁻¹)	61.40 ± 2.70
C _{org} (g kg ⁻¹)	1.44 ± 0.03
Total N (‰)	0.60 ± 0.10
C/N (-)	2.40 ± 0.48
³ OM (%)	2.47 ± 0.05

¹ Values are means ($n = 3$) ± standard errors. ² EC: Electrical Conductivity. ³ OM: Organic Matter.

Biochar applied to soil was produced at the STAR*Facility Centre, Foggia University, from residual vine biomasses (*Vitis vinifera* L.) collected from a local vineyard. The pruning residues (15% humidity) were chipped into particles of approx. 50 mm, mixed and then pyrolyzed at a temperature of 750 °C for 8 h, in a pilot scale with a fixed-bed tubular reactor (30 L capacity). The heating rate was 10 °C min⁻¹. Once cooled, it was ground and passed through a 2 mm sieve.

The pH and electrical conductivity (EC) were determined on a 1:20 (w/v) soil/biochar suspension with deionized water, after shaking and waiting an equilibrium time of 90 min before measurement by a pH meter (GLP 22+ Crison Instruments, Barcelona) and an EC-meter (GLP 31+ Crison Instruments, Barcelona), respectively. The proximate analysis—the fixed carbon, volatile solids, ash and water content—was carried out by a TGA Analyzer (LECO-TGA701). The ultimate analysis of the carbon (C), hydrogen (H) and nitrogen (N) content was performed by dry combustion using a CHN Elemental Analyzer (CHN LECO628). In the case of C_{org}, dry combustion was preceded by inorganic C removal with HCl. Similarly, sulfur (S) was determined using a S module (S LECO628) combined with the CHN Elemental Analyzer. Oxygen (O) was calculated by difference. The carbon stability of biochar was evaluated indirectly by the molar ratios of hydrogen to organic carbon (H/C_{org}) and oxygen to organic carbon (O/C_{org}). The micro- and macro-elements were determined by digesting the dried biochar sample in concentrated HNO₃, in a closed vessel microwave digester (CEM-Mars6). The metals in the solution were then analyzed by inductively coupling plasma optical-emission spectroscopy (ICP-OES Agilent 720). The physicochemical characteristics of the obtained biochar are listed in Table 2. It was char-

acterized by the typical alkaline pH value [48] and resulted in a higher EC than the receiving soil. The prepared biochar fully complied with the standards established by both EBC (European Biochar Certificate) [49] and IBI (International Biochar Initiative) [50] because the C content was higher than 50%, the C_{org} higher than 60%, the H/C_{org} ratio lower than 0.7 and the O/C_{org} ratio lower than 0.4. Taking these properties into account, the available biochar was assigned to the Class 1 grade, while it also offered long-term carbon stability and persistence.

Table 2. Main physicochemical characteristics of biochar added to the soil.

Characteristic	Value ¹		Characteristic	Value ¹	
pH	10.61	± 0.06	Ca (mg kg ⁻¹)	101,986.40	± 1791.84
EC (mS m ⁻¹)	249.00	± 4.84	K (mg kg ⁻¹)	34,358.80	± 1622.78
Fixed carbon (% dw)	74.79	± 0.33	Mg (mg kg ⁻¹)	12,789.57	± 32.75
Volatile solids (% dw)	15.31	± 0.31	P (mg kg ⁻¹)	5479.17	± 169.99
Ash (% dw)	9.90	± 0.04	Fe (mg kg ⁻¹)	4014.62	± 365.69
Water content (% a.r.)	3.35	± 0.03	Si (mg kg ⁻¹)	2868.42	± 586.87
C (% dw)	67.69	± 1.08	S (mg kg ⁻¹)	1914.16	± 49.53
H (% dw)	2.06	± 0.05	Na (mg kg ⁻¹)	1738.70	± 181.87
N (% dw)	1.01	± 0.02	Cu (mg kg ⁻¹)	636.74	± 92.02
S (% dw)	0.18	± 0.01	Zn (mg kg ⁻¹)	240.16	± 3.29
O (% dw)	17.94	± 1.46	Mn (mg kg ⁻¹)	195.21	± 12.32
C_{org}	67.01	± 1.07	H/C_{org} ratio (-)	0.37	± 0.01
C/N	66.19	± 0.28	O/C_{org} ratio (-)	0.20	± 0.02

¹ Values are means ($n = 3$) ± standard errors. dw: dry weight; a.r.: as received.

2.2. Experimental Treatments

Soil and biochar, both dried and sieved, were used to prepare soil–biochar mixtures. Biochar was added to the soil at 0, 2, 4, 6, 8 and 10% rates. The applied formula to set the correct amount of biochar in the mixture was the following:

$$B_i = S \frac{X_i}{100 - X_i} \quad (1)$$

where B is the biochar dry weight, S the soil dry weight, X the percentage of biochar to be added, while subscript i refers to the soil–biochar specific treatment.

Six experimental treatments (soil–biochar mixtures) were arranged as follows: B0 (soil + 0% biochar or control), B2 (soil + 2% biochar), B4 (soil + 4% biochar), B6 (soil + 6% biochar), B8 (soil + 8% biochar) and B10 (soil + 10% biochar).

After soil–biochar mixture preparation, 5 L cylindrical plastic pots (internal $\varnothing = 20$ cm; $h = 16$ cm) were filled with the same mixtures. An equal volume of each soil–biochar mixture was placed in every pot without intentional compaction and each experimental treatment was done three times. Therefore, 18 pots made up the experimental setting to address the bulk-density measurement (Section 2.3) and the infiltration trial (Section 2.7). The other 18 pots (prepared according to the same procedure) were used to extract smaller soil samples to address the pressure plate apparatus (Section 2.4). Moreover, three identical pots were filled with an equal volume of biochar only. All these pots were sealed with a plastic sheet and kept at room temperature (22 ± 0.5 °C) for three months until the experimental tests were performed.

2.3. Bulk Density of Soil–biochar Mixtures

The bulk density of both the soil–biochar mixtures and biochar alone was determined immediately before the start of the hydrological tests. After three months of storage, the soil–biochar mixtures in the pots did not show any kind of shrinkage. By gently trimming at the top it was possible to bring all the pots to full and equal volume without causing any disturbance to the underlying mixture. Pots were weighed and the bulk density (g

cm^{-3}) of each soil–biochar mixture (ρ_m) was determined as the ratio of the net soil–biochar mixture weight to the pot volume. Considering that treatment B0 represented the non-amended soil, its bulk density corresponded to the bulk density of the soil alone (ρ_s), that is, without biochar addition. The same procedure was also applied to the three pots filled with biochar only. In this way, it was possible to estimate the bulk density of biochar alone (ρ_b).

2.4. Water Content of Soil–Biochar Mixtures at Different Water Potentials

A pressure-plate apparatus equipped with a porous ceramic membrane (Soil Moisture Equipment Corp., Santa Barbara, CA) was used to measure water content (ω , g g^{-1}) of soil–biochar mixtures, according to the Richards' method [51]. Samples of an equal volume of dry soil–biochar mixtures were excerpted from the pots using PVC sampling rings ($\text{Ø} = 52 \text{ mm}$; $h = 1 \text{ cm}$; volume = 21 cm^3). On these samples, the bulk density of the soil–biochar mixtures was further calculated in parallel with the procedure already reported in Section 2.3. Then, each sample was saturated with distilled water through partial soaking and by imbibition from below. As soon as saturation was reached, every sample was weighed and then placed on a porous ceramic plate before being placed into the pressure chamber. By using an air compressor, a constant pressure was established inside the chamber. The selected pressure corresponded to a specific value of the assigned matrix potential to be tested. Seven subsequent matric potentials (ψ , kPa), namely, saturation ($\psi = 0 \text{ kPa}$) and $\psi = -10, -30, -50, -100, -500$ and -1500 kPa were selected.

The mixture ring samples were finally weighted and then dried at 105 °C for 24 h.

At every pressure step, the mixture water content was determined gravimetrically with respect to the dried weight. Therefore, the water content at each matric potential was expressed as percentage by weight of the soil–biochar mixtures (ω , g g^{-1}).

The previously determined bulk density of each soil–biochar mixture (ρ_m) allowed converting the water content from a gravimetric (ω , g g^{-1}) to a volumetric basis (θ , $\text{cm}^3 \text{ cm}^{-3}$), according to the following equation:

$$\theta = \omega * \frac{\rho_m}{\rho_w} \quad (2)$$

where ρ_w is the water density currently assumed equal to 0.998 g cm^{-3} at 20 °C .

2.5. Water Capacitive Indicators of Soil–biochar Mixtures

A set of capacity-based soil water indicators [52] was applied to each of the six soil–biochar mixtures to compare their hydraulic properties. These indicators derive directly from the volumetric water contents (θ , $\text{cm}^3 \text{ cm}^{-3}$) previously measured at characteristic matrix potentials, specifically: saturation ($\theta_{\text{SAT}} \rightarrow \psi = 0 \text{ kPa}$), field capacity ($\theta_{\text{FC}} \rightarrow \psi = -10 \text{ kPa}$), matrix capacity ($\theta_{\text{MRX}} \rightarrow \psi = -100 \text{ kPa}$) and wilting point ($\theta_{\text{WP}} \rightarrow \psi = -1500 \text{ kPa}$). It is generally remarked that the threshold value $\psi = -100 \text{ kPa}$ approximately discriminates structural from matric soil pores [53].

Therefore, the following capacitive indicators (Figure 2) were applied:

$$\text{Total available water: TAW (\%)} = (\theta_{\text{SAT}} - \theta_{\text{WP}}) * 100; \quad (3)$$

$$\text{Drainage water: DRW (\%)} = (\theta_{\text{SAT}} - \theta_{\text{FC}}) * 100; \quad (4)$$

$$\text{Plant-available water: PAW (\%)} = (\theta_{\text{FC}} - \theta_{\text{WP}}) * 100; \quad (5)$$

$$\text{Readily available water: RAW (\%)} = (\theta_{\text{FC}} - \theta_{\text{MRX}}) * 100; \quad (6)$$

$$\text{Limited available water: LAW (\%)} = (\theta_{\text{MRX}} - \theta_{\text{WP}}) * 100. \quad (7)$$

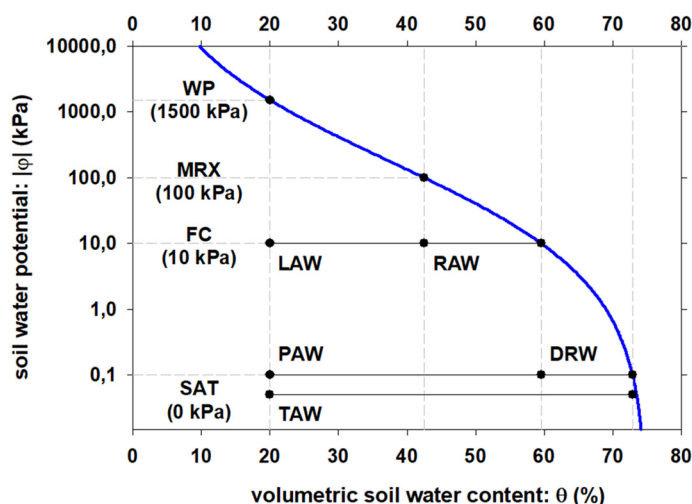


Figure 2. Graphical representation of the soil water capacity indicators (TAW, PAW, DRW, LAW and RAW) as determined by the volumetric water content (%) corresponding to the characteristic water potentials (SAT, FC, MRX and WP) along the soil adsorption curve. (Read the text for explanations of acronyms and initialisms.)

It can be easily observed that:

$$\text{TAW} = \text{DRW} + \text{PAW};$$

$$\text{PAW} = \text{RAW} + \text{LAW};$$

Therefore, the following further relative indicators were applied:

$$\text{Relative available water (\%)}: (\text{PAW}/\text{TAW}) * 100; \quad (8)$$

$$\text{Relative readily available water (\%)}: (\text{RAW}/\text{PAW}) * 100. \quad (9)$$

2.6. Soil Water Desorption Curve of Soil–biochar Mixtures

Water content data on volumetric basis were used to describe the water desorption curve of the six soil–biochar mixtures. For this purpose, the van Genuchten model [54] was fitted to the experimental data by applying the following equation:

$$\theta(\psi) = \theta_r + \frac{\theta_s - \theta_r}{[1 + (\alpha \psi)^n]^m} \quad (10)$$

where: $\theta(\psi)$ is the actual soil water content ($\text{cm}^3 \text{cm}^{-3}$) at the matric potential ψ (kPa); θ_r is the residual soil water content ($\text{cm}^3 \text{cm}^{-3}$) at limit values of matric potential ($\psi \rightarrow \infty$); θ_s is the saturated water content ($\text{cm}^3 \text{cm}^{-3}$), assuming equivalence with total porosity; α is a dimensionless parameter related to the inverse value of the air entry potential (kPa^{-1}); n and m are dimensionless curve shape parameters. In particular, m characterizes the asymmetry of the curve and the Mualem constraint $m = 1 - 1/n$ was applied [55]. Therefore, equation (10) only contains the following four unknown parameters: θ_s , θ_r , α , and n to be determined by a statistical fitting procedure (Section 2.5). Once specific estimates are assigned to the model parameters, further indicators useful in the soil–biochar mixture comparisons are the following:

- matric potential of the inflection point of the water desorption curve (ψ_i , kPa):

$$\psi_i = \frac{1}{\alpha} \left(\frac{n}{1-n} \right)^{\frac{1}{n}} \quad (11)$$

- water content at the inflection point, (θ_i , $\text{cm}^3 \text{cm}^{-3}$):

$$\theta_i = \theta r + (\theta s - \theta r) \left(1 + \frac{1}{m}\right)^m \quad (12)$$

- slope of the water retention curve at the inflection point (S_i):

$$S_i = -n (\theta s - \theta r) \left(\frac{2n-1}{n-1}\right)^{\left(\frac{1}{n}-2\right)} \quad (13)$$

It should be specified that the soil water release or desorption curve is expressed as volumetric water content (θ , $\text{cm}^3 \text{cm}^{-3}$) versus the absolute value of pore water tension (ψ , kPa) is expressed as natural logarithm: $\ln|\psi|$.

The pore volume distribution function, $P(\psi)$, may be defined as the slope (first derivative $d\theta/d\psi$) of the water release curve expressed as volumetric water content θ ($\text{cm}^3 \text{cm}^{-3}$), versus $\ln(\psi)$, and plotted against the equivalent pore diameter, δe (μm), on a logarithmic scale [52]. The equivalent pore diameter (δe) may be determined according to the Young–Laplace equation, and assuming that the pores are perfectly cylindrical, uniform, and equally drained, according to the following formula [41,52]:

$$\delta e = \frac{292}{\psi} \quad (14)$$

with δe (μm) and ψ (kPa)

Therefore, the van Genuchten curves were converted into pore volume distribution functions, and this can be considered the ultimate way to compare the six soil–biochar mixtures with respect to their hydraulic properties.

2.7. Water Infiltration of Soil–biochar Mixtures

Water infiltration in the pots filled with the six soil–biochar mixtures was measured using a mini-disk infiltrometer (Meter Group Inc., Pullman, WA, USA). A constant pressure head of -2 cm was applied [56]. The amount of water (cm) that infiltrated into the soil–biochar mixtures was recorded manually at intervals of 10 s until all water from the reservoir chamber was infiltrated. The infiltration test was applied to every available pot and; therefore, three infiltration measurements were performed for each soil–biochar mixture.

Cumulative infiltration (I_c , cm) was measured over time and the infiltration rate (I_R , cm s^{-1}) was determined as the difference between two cumulative infiltration (I_c) readings over the corresponding time interval (t):

$$I_R = \frac{(I_c)_2 - (I_c)_1}{t_2 - t_1} \quad (15)$$

In particular, three values of average infiltration rate were calculated. The initial infiltration rate ($I_{R\text{start}}$) was determined over the first 60 s of the infiltration run, the final infiltration rate ($I_{R\text{end}}$) determined over the last 60 s of the infiltration run and, finally, the total infiltration rate ($I_{R\text{total}}$), determined as the ratio of the total infiltrated water volume over the total time of the experimental infiltration process.

Cumulative infiltration (I_c) data were analyzed by fitting the Philip's infiltration model [56–58], as follows:

$$I_c = C_1 \sqrt{t} + C_2 t \quad (16)$$

where: I_c (cm) is the cumulative infiltration; C_1 ($\text{cm/s}^{1/2}$) is the soil sorptivity; C_2 (cm/s) is the parameter related to soil hydraulic conductivity; t is the time (s). A mathematical fitting procedure was applied to estimate the two coefficients, C_1 and C_2 , and their assigned values were used as further indicators to compare the hydraulic properties of the soil–biochar mixtures. The instantaneous infiltration rate was determined by differentiating, with respect to time, the cumulative infiltration as reported in the following equation:

$$I_R = 0.5 C_1/\sqrt{t} + C_2 \quad (17)$$

2.8. Statistical Analysis

The soil–biochar bulk-density data were processed according to an ANCOVA model considering the biochar addition rate (from zero to 10%) as the regressing variable. Both “expected” and “observed” data were the response variables. The former being the data theoretically compatible with a simple “dilution” effect of biochar in the mixtures, while the latter the actually measured data. In other words, a “lighter” component (the lower density biochar) when added to a “heavier” medium (the higher density soil) produced a decrease in the mixture bulk density proportional to the amount (weight) of the added component, according to the following equation:

$$\rho_{m(i)} = \rho_s (100-X_i)/100 + \rho_b X/100 \quad (18)$$

where, as already stated, X is the percentage of the added biochar, while the subscript i refers to the soil–biochar specific treatment. According to equation (18), the expected values of bulk density can be calculated. Therefore, the ANCOVA model allowed testing if the decreasing effect of biochar on bulk density (i.e., the slope of the regression line) was statistically different in the two compared data sets (expected vs. observed).

A one-way ANOVA test was applied to statistical process all the water-capacitive indicators as well as the average infiltration rates with respect to the experimental treatments (the six soil–biochar mixtures). A mean comparison was performed via a Tukey honestly significant difference (HSD) test, and a 0.05 probability level was applied. A multivariate analysis was also performed on the water-capacitive indicators, which were processed as a whole through a cluster analysis. The “average linkage method” was applied, and the resulting dendrogram was represented considering the detected clusters.

The parameter estimates of the two models, van Genuchten and Philip’s, were obtained through an iterative, nonlinear, least-square fitting procedure. In this respect, a “stepwise” approach was applied according to the following procedure:

1. The model was fitted independently to the data from every experimental B_i treatment (from B0 to B10) to obtain specific parameter estimates. The overall experimental error (SSE—Sum of Square error) was obtained as the sum of SSE related to each treatment curve ($\sum SS_i$).
2. The model was then fitted to the complete dataset, regardless of experimental treatments, to obtain a single, general estimate of each model parameter.
3. The general model (point 2) was gradually relaxed, one parameter at a time, keeping the others fixed. The statistical significance of an independent estimates of each B_i treatment i was evaluated, one parameter at a time, by means of an F Fisher test against the error term (SSE).
4. We proceeded with point 3 in order of relevance, from the most to the least influential parameter. The additional SS, accounted for by the model when fitting B_i -independent estimates of each parameter, represented its relevance.
5. A significant F-test allowed the conversion of the model from one single estimate of the considered parameter to different estimates, according to a multiple range comparison among the B_i treatments. A non-significant F-test allowed the preservation of a unique estimate of the considered parameter.
6. The same procedure was repeated each time considering the remaining model parameters; every time, a new fitting procedure assigned new estimates to the remaining parameters.

All data processing and statistical tests were performed using the JMP statistical software package, version 11 (SAS Institute Inc, Cary, NC, USA).

3. Results and Discussion

3.1. Bulk Density of Soil–biochar Mixtures

Two independent and parallel bulk-density estimates of the six soil–biochar mixtures were obtained. The first estimates derived from weighing the entire pots (Section 2.3), while the second from weighing the smaller ring samples placed in the pressure-plate apparatus (Section 2.4). No statistical differences were detected between the two datasets (data not showed). Since the first estimates came from a greater volume of mixtures (the pots) than the second ones (ring samples), the former were considered more reliable and taken as a reference.

The bulk density of the soil–biochar mixtures decreased linearly with the biochar fraction added to the soil (Figure 3).

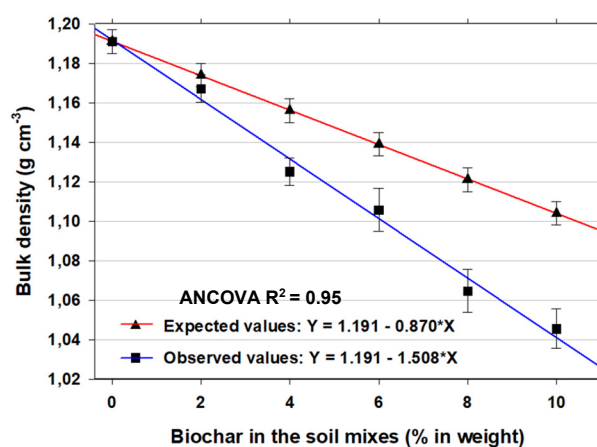


Figure 3. Linear regression of bulk density (g cm^{-3}) against increasing fractions (%) of biochar in the soil to obtain the experimental soil–biochar mixtures. Red line represents the expected trend based on a simple “dilution” effect, while the blue line regressed the observed data as experimentally observed. The slopes of the two lines are significantly different according to the ANCOVA results. Vertical bars are standard errors.

Our results were consistent with other experimental studies [1] as well as meta-analysis [59]. Most studies showed a reduction in bulk density as a consequence of biochar addition although few cases also reported increase in bulk density [17]. A biochar addition roughly higher than 2% by weight should be enough to create a significant decrease in bulk density [60]. The rate of biochar application as well as the density and porosity of the original soil are critical for predicting the effects of a biochar addition to soil. In our experiment, the biochar bulk density was $0.321 \pm 0.074 \text{ g cm}^{-3}$, while the soil bulk density was 1.191 ± 0.079 . Therefore, considering an addition of biochar (10% by weight), a bulk density decrease of 12.6% was actually detected compared to an expected decrease of 7.3% if only a “dilution” effect were supposed. This decrease, therefore, does not follow the proportions resulting from a simple “dilution” effect (red line in Figure 3) since the reduction observed (blue line in Figure 3) was significantly stronger than expected. This was proved by the result of the ANCOVA test reported in Table 3.

Table 3. Results of the ANCOVA test performed on the expected and observed bulk density values of the six soil–biochar mixtures.

Source of Variation	Estimate	Std Err	Prob
Intercept	1.191	0.001	<0.0001
Average slope	−1.189	0.023	<0.0001
Expected vs. Observed	−0.319	0.014	<0.0001

As far as we know, only one other paper [53] compared the expected “dilution” data with the actual observed data of bulk density, thereby showing that the effect of biochar in reducing the soil bulk density was more than proportional to the simple contribution of its weight. Consequently, it is appropriate to call into question the effects of the spatial arrangement of biochar particles in relation to soil particles or small aggregates. This implies an increase in total porosity not only due to the intrinsic biochar microporosity, but also due to a soil–biochar interporosity. Apart from reasons of simple particle spatial arrangement, the effect of soil–biochar interaction may also lead to the development of structural aggregates. Considering that biochar increases the mixture cation exchange capacity (CEC), the bridging of clays and organic matter may be promoted; on the other hand, the increase in soil reaction (pH) may also increase surface nonacidic cations bridging soil colloids [53]. A better particle aggregation may promote soil structuring and a decrease in bulk density. Considering the limited time available for soil structuring in this experiment, we believe the former factor should be more effective than the latter.

3.2. Water Capacitive Indicators of Soil–Biochar Mixtures

The one way ANOVA test performed on each capacitive indicator (Table 4) gave quite clear results concerning the different hydraulic properties of the six soil–biochar mixtures. TAW, PAW, RAW, and LAW increased progressively with increasing biochar application fractions; conversely, DRW decreased. In general, biochar effectively contributed to improved soil quality with respect to water plant–soil relationships. When comparing the maximum range between treatment pairs, water holding capacity (TAW) and water availability to plants (PAW, RAW and LAW) increased significantly. Mostly importantly, the highest increase was observed in RAW (+73%), followed by PAW (+61%) and LAW (+54%), while DRW was reduced by approximately 46%. Not only the amount of available water to plants was significantly expanded, but also the amount of drainage water (lost water or only temporary available to plants) was significantly reduced. Concerning the relative indicators, PAW/TAW grew significantly larger with the biochar addition (+32%, the maximum range between treatment pairs), while RAW/PAW did not significantly change.

Table 4. Capacitive indicators (%) for the six soil–biochar mixtures (treatments).

Treat ment	TAW	DRW	PAW	RAW	LAW	PAW/TAW	RAW/PAW
B0	41.95 c	14.74 a	27.21 b	17.48 b	9.73 b	65.06 b	64.19 a
B2	43.82 c	14.46 a	29.36 b	18.72 b	10.64 b	67.02 b	63.76 a
B4	45.01 bc	15.02 a	29.99 b	19.23 b	10.76 b	66.70 b	64.12 a
B6	49.81 ab	8.93 ab	40.88 a	26.99 a	13.88 a	82.05 a	65.97 a
B8	51.00 a	7.18 b	43.82 a	30.29 a	13.53 a	85.93 a	69.10 a
B10	51.62 a	7.97 b	43.65 a	28.71 a	14.94 a	84.73 a	65.73 a
Std Error	1.09	1.33	0.83	0.89	0.40	2.30	1.26
CV (%)	2.31	11.68	2.32	3.78	3.26	3.06	1.92

Within columns, means followed by the same letter are not significantly different via Tukey HSD at $\alpha = 0.05$.

Several experimental evaluations [17], both in the field and in the lab, demonstrated that soil amendment with biochar is associated with a significant increase in PAW. The magnitude of this increase is related to the soil’s being higher in coarse-textured and lower in fine-textured soils, as well as roughly proportional to the biochar application rate. Similar to what was previously observed with bulk density, this effect is mostly interpreted in reference to a remarkable increase in the total soil porosity and specific surface area [59]. According to the same meta-analysis [59] the effect of biochar on PAW increases as

its porosity increases. Biochar has been seen to increase not only total soil porosity but also pore connectivity and the number of pores [61,62], thus increasing soil water retention. As remarked already, biochar intrapores (pores inside the biochar particles) together with soil–biochar interpores jointly contribute to increasing water retention [63]. According to our results, the increase in PAW due to the biochar addition was mostly determined by a significant increase in water content at FC (+27.9%, the maximum range between treatment pairs).

The treatment with the highest biochar fraction did not always show the most noticeable results; indeed, with respect to PAW and RAW, it was B8, not B10, that offered the best soil conditions although it was not statistically different. A sort of “threshold effect” in biochar application was detected in this lab experiment. Interestingly, the same effect was also observed in our previous field-conducted experiment [13]. Indeed, B8 and B10 showed a general trend (not statistically confirmed) to swap places. This was particularly clear when the result of the cluster analysis jointly applied to all the data reported in Table 4 are shown (Figure 4). A clear split into two clusters (B0–B2–B4 vs. B6–B8–B10) was shown. Moreover, a closer “friendship” between B6 and B10 rather than B8 and B10 was observed. It is difficult to provide an explanation of the observed swapping between B10 and B8, but it seemed that no further porosity was added to the mixture; that is to say, the “useful” porosity to the plant water supply was partially lost in B10 with respect to B8.

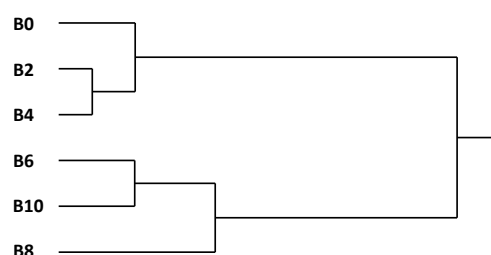


Figure 4. Cluster analysis (average linkage method) applied on data reported in Table 4. A clear split into two clusters (B0–B2–B4 vs. B6–B8–B10) is shown. Moreover, a closer “friendship” between B6 and B10 rather than B8 and B10 can be observed. This particular behavior suggests a possible threshold effect of biochar application to soil. (Read the text for an in-depth explanation).

3.3. Water Retention Curves of Soil–Biochar Mixtures

The fitting procedure of the van Genuchten equation, performed according to a “stepwise” approach, provided a model consisting of only two curves significantly different from each other. The first curve included the following treatments: B0, B2 and B4, while the second one the other three treatments: B6, B8 and B10. The pair of curves differed significantly in the value of θ_s and n (Table 5), while neither α nor θ_r had statistically different results among the B_i treatments (Table 5). In particular, θ_r never differed significantly from zero in any B_i treatment, and for this reason its value was zeroed (Table 5).

Table 5. Results of the “stepwise” procedure applied in performing the parameter fitting of the van Genuchten model to the six soil–biochar mixtures (B_i treatments). Standard error of the estimates, together with their confidence intervals at 95% of probability are also reported.

Parameter	Treatment	Estimate	Std Err	Lower Conf.	Upper Conf.	
θ_s (%)	B0, B2, B4	69.18	0.44	68.30	70.07	b
	B6, B8, B10	75.08	0.56	73.97	76.19	a
n (-)	B0, B2, B4	1.38	0.01	1.35	1.41	b
	B6, B8, B10	1.47	0.02	1.44	1.51	a
α (kPa ⁻¹)	B6, B8, B10	0.0066	0.0004	0.0058	0.0075	<i>n.s.</i>
	B0, B2, B4	0.0057	0.0004	0.0050	0.0064	
θ_r (%)	All B_i	0,000	-	-	-	

The most influential effects of biochar application was a significant increase in the total volume of water at saturation (θ_s). As a consequence, the soil water content also increased at lower water potentials, thus improving plant water availability. The increase in the value of the n parameter further operated in this direction. Indeed, the increase in the n “shape” parameter accentuated the steepness of the curve, simultaneously increasing the water volume at FC and, by contrast, decreasing it at WP. Consequently, a remarkable increase in PAW was obtained and this effect represented another relevant result of biochar application: a significant enhanced capacity of the amended soil to hold water not only at soil saturation but also at unsaturated soil conditions.

Beyond the rigorous statistical separation performed with the “stepwise” approach, both θ_s and n showed a gradual, progressive increase in their values from B0 to B10 (Table 6). In contrast, no kind of trend was detected with respect to the α parameter (Table 6).

Table 6. Estimates of the van Genuchten model parameters to the six soil–biochar mixtures (treatments) without the clustering operations applied in the stepwise approach. (Compare Table 6 with Table 5).

Treatment	θ_s	Std Err	n	Std Err	α	Std Err
B0	67.48	0.80	1.34	0.02	0.0065	0.0007
B2	69.56	0.72	1.39	0.02	0.0055	0.0006
B4	70.51	0.70	1.41	0.03	0.0051	0.0005
B6	73.51	0.76	1.45	0.03	0.0076	0.0008
B8	75.17	1.00	1.49	0.03	0.0067	0.0007
B10	76.56	0.96	1.49	0.03	0.0056	0.0006

The effect of the biochar application on both θ_s and n allowed us to deduce that its main consequence is a substantial, additional contribution to soil porosity that can increase water sorption capacity. While the increasing trend on θ_s seemed quite regular, the values related to the n parameter reached a maximum at B8 and did not increase at B10, thus limiting any further increase in soil water-holding capacity (Table 6). Again, as previously noticed, a peculiar effect of biochar at a higher application rate (although not statistically confirmed) was observed.

According to the statistical results reported in Table 5, Figure 5A shows the two desorption curves with respect to the first (B0, B2 and B4) and the second (B6, B8, B10) group of treatments. The two curves differed significantly, visually confirming what was previously observed with regard to the capacitive indicators and the van Genuchten parameters. They showed similar values around and beyond water potential (WP) (N.B.: ψ in absolute terms); conversely, they showed a divergent trend at increasingly lower water potentials (N.B.: ψ in absolute terms), in the range of PAW as well of DRW.

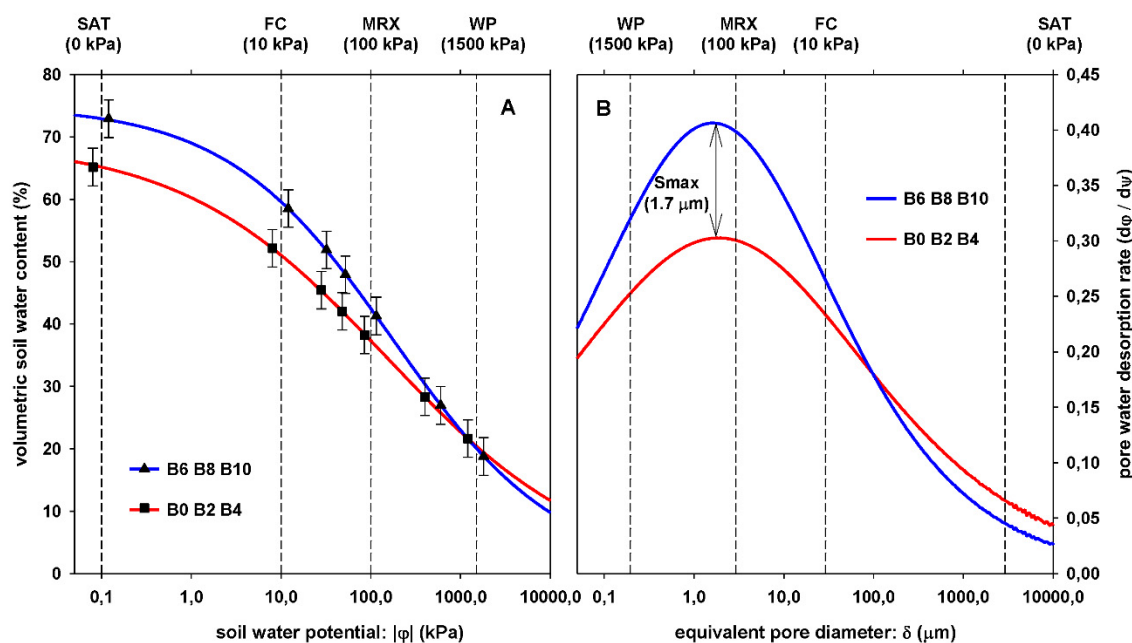


Figure 5. (A) Desorption curves of the two statistically different treatment clusters (B0, B2 and B4) vs. (B6, B8 and B10) according to the van Genuchten model. (B) pore size distribution functions of the same former curves, obtained by calculating their slope (first derivative $d\theta/d\psi$) and plotting the data on an x -axis where soil water potential values were converted into pore equivalent diameter.

Figure 5B represents, even more clearly, the conditions occurring in the soil as a consequence of biochar addition from lower (B0, B2 and B4) to higher quantities (B6, B8, B10). What could be observed in the pore-size distribution of the soil–biochar mixtures was a significant increase in that fraction of porosity straddling the size of the pores that marks the transition from “matrix” porosity (intra-aggregate voids) to “structural” porosity (interaggregate voids). Indeed, among aggregates, pores are formed that hold water primarily by capillary forces associated with the clumping of aggregates; these can be termed “structural” pores. In contrast, “matrix” pores are intra-aggregate, formed among elementary textural particles where interparticle adhesive forces principally hold water. In this respect, it is usually assumed that the former fraction of soil water is more easily available for the plant than the latter.

The inflection points of the two curves in Figure 5A corresponded to the maximum value of the two curves in Figure 5B. They represented the slope of the water-retention curves at their respective inflection points (S_i). The S_i value was significantly higher in the blue line (B6, B8, B10) than in the red one (B0, B2 and B4), although they were both achieved at exactly the same water potential (170 kPa), corresponding to an equivalent pore size equal to 1.72 μm . As expected, the soil water content at the inflection point (θ_i) was higher in the blue line (B6, B8, B10) than in the red one (B0, B2 and B4), further stressing the improved soil quality offered by biochar application with respect to soil–water relationships.

The symmetry observed in the two pore size-distribution curves suggests that biochar addition at higher rates did not produce a curve shifting and significantly increased the amount of the existing pore classes, both intra- and inter-aggregates (i.e., at both sides of MRX, see Figure 5B). This general increase in porosity can explain both the reduction in bulk density of the mixtures, which was more than proportional to the bulk density of the added biochar, and the increase in the mixture water-retention capacity. Indeed, the first effect can be predominantly accounted for by the increase in the structural (interaggregate) porosity, while the second effect can be predominantly associated with interporosity with respect to RAW and intraporosity with respect to LAW. Adding RAW and LAW gives PAW.

If we consider that the peak of the two curves in Figure 5B roughly corresponds to the edge that separates the micro- from the meso-porosity, it is possible to understand the beneficial effect exerted by the addition of biochar in favouring water retention, precisely at the most convenient potentials for plant-water uptake (i.e., those in the range WP–FC).

3.4. Water Infiltration of Soil–Biochar Mixtures

The average infiltration rate of water into the six different soil–biochar mixtures showed decreasing values as the biochar application rates from B0 to B10 (Table 7) increased. This trend was observed with respect to the initial (first 60 s of the process), the final (last 60 s) and the total average value of infiltration rates (the entire process duration). Considering the B8 treatment, a lower value for the final and total rate was detected compared to that of B10. From a statistical perspective, the ANOVA results determined only two distinct treatment groups, namely, the first, represented by only the B0 treatment, and the second, which comprises all other treatments (Table 7).

Table 7. Average infiltration rates (I_R cm sec^{−1}) in the soil–biochar mixtures (treatments) at the beginning (first 60 s), at the end (last 60 s) and for the entire duration of the process.

Treatment	IR Initial		IR Final		IR Total	
B0	0.0381	a	0.0220	a	0.0281	a
B2	0.0248	b	0.0134	b	0.0158	b
B4	0.0243	b	0.0124	b	0.0150	b
B6	0.0225	b	0.0108	b	0.0136	b
B8	0.0215	b	0.0098	b	0.0125	b
B10	0.0210	b	0.0105	b	0.0130	b
Std Err	0.0013		0.0015		0.0012	
CV (%)	5.13		11.32		7.35	

Within columns, means followed by the same letter are not significantly different via Tukey HSD at $\alpha = 0.05$

The ANCOVA model, applied to the infiltration data in order to estimate the coefficients of the Philip’s model, confirmed the same statistical results shown in Table 7; the two model coefficients, C1 and C2, were significantly affected by the biochar presence or absence but not significantly by the biochar amount (Table 8).

Table 8. Results of the stepwise procedure in application of the Philip’s cumulative infiltration model to the six soil–biochar mixtures. Biochar treatments (B2, B4, B6, B8 and B10) were grouped because they were not statistically different from each other. B0 remained statistically separated from the other treatments. The standard error of the estimates, together with their confidence intervals at 95% of probability are also reported.

Source of Variation	Estimate	Std Err	Lower Conf	Upper Conf	
C ₁ : [X = sqrt (time)]	0.1531	0.0090	0.1355	0.1706	**
Treat [No Biochar]	+0.0249	0.0090	0.0074	0.0425	a
Treat [Biochar]	−0.0249	0.0090	−0.0425	−0.0074	b
C ₂ : [X ² = time]	0.0116	0.0008	0.0101	0.0131	**
Treat [No Biochar]	+0.0033	0.0008	0.0018	0.0048	a
Treat [Biochar]	−0.0033	0.0008	−0.0048	−0.0018	b

Within columns, means followed by the same letter are not significantly different via Tukey HSD at $\alpha = 0.05$. **, F test significant at $p \leq 0.01$.

Both the “sorptivity” coefficient (C₁) and the “conductivity” coefficient (C₂), showed higher values in soils without biochar application and lower values when biochar was added, regardless of the biochar amount applied. These values fully confirmed the results of the ANOVA test performed on the initial, final and total average infiltration rates, as reported in Table 6.

The application of the Philip's model considering both the cumulative infiltration and the instantaneous infiltration rate is represented in Figure 6.

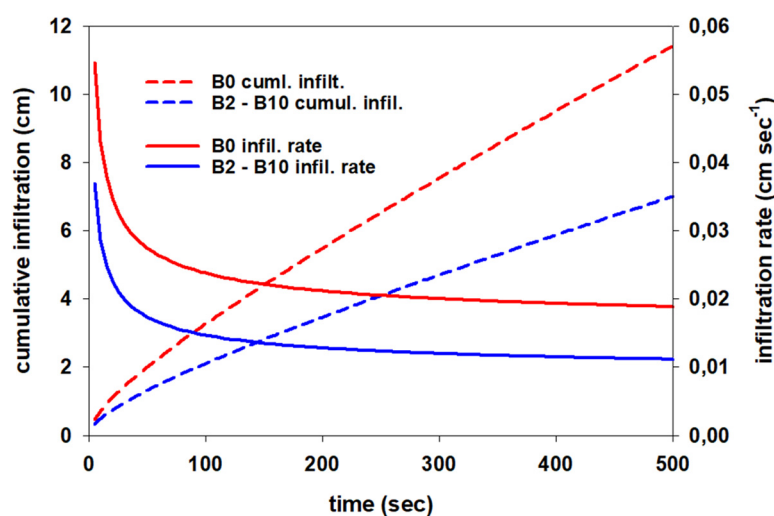


Figure 6. Cumulative infiltration (dashed lines) and instantaneous infiltration rate (solid line) derived from the application of the Philip's model. Biochar treatments (B2, B4, B6, B8 and B10) were grouped because they were not statistically different from each other. B0 remained statistically separated from the other treatments.

Considering equation (16), the first-term of the model (controlled by the “sorptivity” coefficient C_1) strongly dominated the process at the initial stage of infiltration. At this stage the soils were almost dried and the capillary and matrix forces at the soil pore surfaces largely prevailed over the gravitational forces because the larger pores were still empty. Therefore, vertical water movement proceeded at almost the same rate as horizontal water movement. The “gravity” component, controlled by the second term of the model (the “conductivity” coefficient C_2), exerted a negligible effect at the very beginning of the infiltration process, but became progressively more important as infiltration proceeded and the soils became wetter. Finally, the second term of the Philip's equation strongly dominated the process when the soils were almost under saturated condition and the gravitational forces exerted a prevailing effect, while capillarity and matrix forces were, this time, negligible.

Considering the overall infiltration results (Tables 7 and 8 and Figure 6), it appeared that the predominant effect was the presence or absence of biochar, rather than the quantity added to soil. Biochar slowed infiltration into the soil compared to soil without biochar applied. This effect was significantly greater than the effect exerted by the different biochar concentrations in the soil. These results are not in agreement with those generally observed in fine- and fine-loam soils. According to a review paper [1], biochar application to a fine-textured soils at 5 and 10% by weight increased unsaturated hydraulic conductivity at all matric potentials and generally increased water infiltration. According to the same review [1], the application of biochar to fine-textured soils can improve water flow (both infiltration and hydraulic conductivity) because of an increase in pore volume and an improved soil aggregation. It is generally recognized that the addition of biochar significantly enhanced the formation of macro-aggregates that slightly increased the saturated hydraulic conductivity of the amended soils [64]. However, it should be remembered that in our experiment a sieved and repacked soil was used, and these particular conditions may have profoundly affected the results, which would be very different if the soil had been in situ. Indeed, it was also observed [59] that, as a general trend, biochar addition reduced soil-saturated hydraulic conductivity in laboratory experiments compared to those in field studies but without considering specific soil textures. It should be

expected that under our lab experiment there was neither the time nor the proper conditions to promote the development of a good soil structure with macro-aggregates because of the contribution of biochar as a soil amendment.

Concerning the effects displayed by the biochar application to soil, on the one hand, the augmented intraporesity conferred by biochar (with small pore size) significantly reduced soil water conductivity when soil was wet and almost saturated [27]. On the other hand, when the soil was still almost dry, we can suppose that biochar showed its hydrophobic property, thus exerting a water-repellent action that significantly reduced the matrix and capillary effect of water attraction by pores and surfaces. This could be the reason that the “sorptivity” coefficient was lower in biochar rather than in the non-amended soil. Biochar hydrophobicity has been largely discussed in the literature [1,33,35]. It was observed, indeed, that biochar’s microstructure is often highly hydrophobic, suggesting that when added to soil it can induce water repellency. This higher water repellency, in turn, can be the possible explanation for reduced infiltration and hydraulic conductivity. It was also observed that, over time, the biochar in the soil *in situ* undergoes oxidation involving organic compounds on the surface of biochar particles. These oxidations can progressively mitigate biochar’s hydrophobic property [1], thus favoring the restoration of higher water conductivity. Results from the literature indicate that “aged” biochar is more hydrophilic than “fresh” biochar and that after additional wetting/drying treatments biochar become less hydrophobic [65–67].

4. Conclusions

The results obtained from a lab experiment with soil in pots confirmed that biochar has the potential to improve the hydrological properties of clay loam soil. We observed, on the one hand, a substantial increase in water retention capacity; on the other, a reduced water infiltration rate. The first effect agrees with the majority of experimental evidence retrieved from the literature, while the second one is somehow not aligned with the prevailing literature. Our interpretation is based on the relevant increase in porosity (intrapore and interpore) that biochar addition brings to soil, permitting higher water adsorption. The altered soil structural condition, the limited time elapsed between biochar application and the experimental measurements, together with the storage of the soil in pots under a sealed covering, prevented the development of macrostructural soil aggregates able to generate larger pores and facilitate internal water fluxes. Furthermore, water infiltration and its conductivity were hampered by the hydrophobic action exerted by “fresh” biochar (i.e., obtained only recently by pyrolysis and applied to the soil).

The positive effect on water-holding capacity showed that biochar has the potential to effectively improve the water available for plants and contribute to reducing the frequency and volume of irrigation in fine-textured soils. These aspects are of great agronomic relevance and can be confirmed in “open field” conditions, too.

The observed effects of biochar with respect to slower water infiltration and limited water conductivity, if confirmed under “open field” conditions, may have a dual consequence. When water infiltration is hindered, the risk of water runoff and soil erosion strongly increases, as does possible waterlogging; this is a negative factor. Conversely, a reduced water movement due to limited hydraulic conductivity significantly slows deep water drainage and consequent nutrient loss through leaching, the latter being a positive factor. Which of the two should be considered as the prevailing factor and which kind of tradeoff should be established largely depends on the environmental farming conditions and operations. Therefore, further experiments under field conditions are needed to clarify these aspects.

Particularly in agricultural regions characterized by climatic water shortage and frequently droughts, such as the Mediterranean, greater water availability and reduced water loss through drainage or runoff due to biochar application could have an agronomic benefit that is perfectly in line with the sustainable management of water resources for irrigation.

Author Contributions: Conceptualization, A.L. and M.M.; methodology, A.L. and M.M.; formal analysis, A.L., M.F. and M.M.; investigation, A.L. and M.M.; data curation, A.L., M.F. and M.M.; writing—original draft preparation, A.L. and M.M.; writing—review and editing, A.L. and M.M.; visualization, A.L. and M.M.; supervision, A.L. and M.M. All authors have read and agreed to the published version of the manuscript.

Funding: This research received no external funding.

Institutional Review Board Statement: Not applicable.

Informed Consent Statement: Not applicable.

Data Availability Statement: The data presented in this study are available on request from the corresponding author.

Acknowledgments: The authors are grateful to Teresa Gentile and Valentina Del Vento for the technical assistance in the laboratory experiment and analyses.

Conflicts of Interest: The authors declare no conflict of interest.

References

- Blanco-Canqui, H. Biochar and soil physical properties. *Soil Sci. Soc. Am. J.* **2017**, *81*, 687–711.
- Ding, Y.; Liu, Y.; Liu, S.; Huang, X.; Li, Z.; Tan, X.; Zeng, G.; Zhou, L. Potential benefits of biochar in agricultural soils: A Review. *Pedosphere* **2017**, *27*, 645–661.
- Kavitha, B.; Reddy, P.V.L.; Kim, B.; Lee, S.S.; Pandey, S.K.; Kim, K.H. Benefits and limitations of biochar amendment in agricultural soils: A review. *J. Environ. Manag.* **2018**, *227*, 146–154.
- Semida, W.M.; Beheiry, H.R.; Setamou, M.; Simpson, C.R.; Abd El-Mageed, T.A.; Rady, M.M.; Nelson, S.D. Biochar implications for sustainable agriculture and environment: A review. *S. Afr. J. Bot.* **2019**, *127*, 333–347.
- Zabaniotou, A.; Rovas, D.; Libutti, A.; Monteleone, M. Boosting circular economy and closing the loop in agriculture: Case study of a small-scale pyrolysis-biochar based system integrated in an olive farm in symbiosis with an olive mill. *Environ. Dev.* **2015**, *14*, 22–36.
- Monlau, F.; Francavilla, M.; Sambusiti, C.; Antoniou, N.; Solhy, A.; Libutti, A.; Zabaniotou, A.; Barakat, A.; Monteleone, M. Toward a functional integration of anaerobic digestion and pyrolysis for a sustainable resource management. Comparison between solid-digestate and its derived pyrochar as soil amendment. *Appl. Energy* **2016**, *169*, 652–662.
- Zabaniotou, A.; Rovas, D.; Delivand, M.K.; Francavilla, M.; Libutti, A.; Cammerino, A.R.B.; Monteleone, M. Conceptual vision of bioenergy sector development in Mediterranean regions based on decentralized thermochemical systems. *Sustain. Energy Technol. Assess.* **2017**, *23*, 33–47.
- Wolf, D.; Amonette, J.E.; Street-Perrott, F.A.; Lehmann, J.; Joseph, S. Sustainable biochar to mitigate global climate change. *Nat. Commun.* **2010**, *1*, 56.
- Wang, J.; Xiong, Z.; Kuzyakov, K. Biochar stability in soil: Meta-analysis of decomposition and priming effects. *GCB Bioenergy* **2015**, *8*, 512–523.
- Agegnehu, G.; Nelson, N.; Bird, M.I. Crop yield, plant nutrient uptake and soil physicochemical properties under organic soil amendments and nitrogen fertilization on nitisols. *Soil Tillage Res.* **2016**, *160*, 1–13.
- Demiraj, E.; Libutti, A.; Malltezi, J.; Rroço, E.; Brahuishi, F.; Monteleone, M.; Sulçe, S. Effect of organic amendments on nitrate leaching mitigation in a sandy loam soil of Shkodra district, Albania. *Ital. J. Agron.* **2018**, *13*, 1136.
- Libutti, A.; Mucci, M.; Francavilla, M.; Monteleone, M. Effect of biochar amendment on nitrate retention in a silty clay loam soil. *Ital. J. Agron.* **2016**, *11*, 273–276.
- Libutti, A.; Cammerino, A.R.B.; Francavilla, M.; Monteleone, M. Soil amendment with biochar affects water drainage and nutrient losses by leaching: Experimental evidence under field-grown conditions. *Agronomy* **2019**, *9*, 758.
- Zhang, C.; Zeng, G.; Huang, D.; Lai, C.; Chen, M.; Cheng, M.; Tang, W.; Tang, L.; Dong, H.; Huang, B.; Tan, X.; et al. Biochar for environmental management: Mitigating greenhouse gas emissions, contaminant treatment, and potential negative impacts. *Chem. Eng. J.* **2019**, *373*, 902–922.
- Wang, S.; Gao, B.; Zimmerman, A.R.; Li, Y.; Ma, L.; Harris, W.G.; Migliaccio, K.W. Physicochemical and sorptive properties of biochars derived from woody and herbaceous biomass. *Chemosphere* **2015**, *134*, 257–262.
- Herath, H.M.S.K.; Camps-Arbestain, M.; Hedley, M. Effect of biochar on soil physical properties in two contrasting soils: An Alfisol and an Andisol. *Geoderma* **2013**, *209–210*, 188–197.
- Omondi, M.O.; Xia, X.; Nahayo, A.; Liu, X.; Korai, P.K.; Pan, G. Quantification of biochar effects on soil hydrological properties using meta-analysis of literature data. *Geoderma* **2016**, *274*, 28–34.
- Głąb, T.; Palmowska, J.; Zaleski, T.; Gondek, K. Effect of biochar application on soil hydrological properties and physical quality of sandy soil. *Geoderma* **2016**, *281*, 11–20.
- Hansen, V.; Nielsen, H.H.; Petersen, C.T.; Mikkelsen, T.N.; Stöver, D.M. Effects of gasification biochar on plant-available water capacity and plant growth in two contrasting soil types. *Soil Tillage Res.* **2016**, *161*, 1–9.

20. Xiao, Q.; Zhu, L.; Zhang, H.; Li, X.; Shen, Y.; Li, S. Soil amendment with biochar increases maize yields in a semi-arid region by improving soil quality and root growth. *Crop Pasture Sci.* **2016**, *67*, 495–507.
21. Yang, C.D.; Lu, S.G. Effects of five different biochars on aggregation, water retention and mechanical properties of paddy soil: A field experiment of three-season crops. *Soil Till. Res.* **2021**, *205*, 104798.
22. Carvalho, M.; Madari, B.; Bastiaans, L.; Oort, P.V.; Leal, W.; Heinemann, A.; da Silva, M.A.S.; Maia, A.H.N.; Parson, D.; Meinke, H. Properties of a clay soil from 1.5 to 3.5 years after biochar application and the impact on rice yield. *Geoderma* **2016**, *276*, 7–18.
23. Wang, D.; Li, C.; Parikh, S.J.; Scow, K.M. Impact of biochar on water retention of two agricultural soils—A multi-scale analysis. *Geoderma* **2019**, *340*, 185–191.
24. Burrell, L.D.; Zehetner, F.; Rampazzo, N.; Wimmer, B.; Soja, G. Long-term effects of biochar on soil physical properties. *Geoderma* **2016**, *282*, 96–102.
25. Uzoma, K.C.; Inoue, M.; Andry, H.; Zahoor, A.; Nishihara, E. Influence of biochar application on sandy soil hydraulic properties and nutrient retention. *J. Food Agric. Environ.* **2011**, *9*, 1137–1143.
26. Zhang, J.; Chen, Q.; You, C.F. Biochar effect on water evaporation and hydraulic conductivity in sandy soil. *Pedosphere* **2016**, *26*, 265–272.
27. Lim, T.J.; Spokas, K.A.; Feyereisen, G.; Novak, J.M. Predicting the impact of biochar additions on soil hydraulic properties. *Chemosphere* **2016**, *142*, 136–144.
28. Ajayi, A.; Horn, R. Modification of chemical and hydrophysical properties of two texturally differentiated soils due to varying magnitudes of added biochar. *Soil Tillage Res.* **2016**, *164*, 34–44.
29. Barnes, R.T.; Gallaghe, M.E.; Masiello, C.A.; Liu, Z.; Dugan, B. Biochar induced changes in soil hydraulic conductivity and dissolved nutrient fluxes constrained by laboratory experiments. *PLoS ONE* **2014**, *9*, e108340.
30. Asai, H.; Samson, B.K.; Stephan, H.M.; Songyikhangsuthor, K.; Homma, K.; Kiyono, Y.; Inoue, Y.; Shiraiwa, T.; Horie, T. Biochar amendment techniques for upland rice production in Northern Laos. *Field Crops Res.* **2009**, *111*, 81–84.
31. Major, J.; Lehmann, J.; Rondon, M.; Goodale, C. Fate of soil-applied black carbon: Downward migration, leaching and soil respiration. *Glob. Chang. Biol.* **2010**, *16*, 1366–1379.
32. Kameyama, K.; Miyamoto, T.; Shiono, T.; Shinogi, Y. Influence of sugarcane bagasse-derived biochar application on nitrate leaching in calcareous dark red soil. *J. Environ. Qual.* **2012**, *41*, 1131–1137.
33. Githinji, L. Effect of biochar application rate on soil physical and hydraulic properties of a sandy loam. *Arch. Agron. Soil Sci.* **2014**, *60*, 457–470.
34. Gray, M.; Johnson, M.G.; Dragila, M.I. Water uptake in biochars: The roles of porosity and hydrophobicity. *Biomass Bioenergy* **2014**, *61*, 196–205.
35. Kinney, T.J.; Masiello, C.A.; Dugan, B.; Hockaday, W.C.; Dean, M.R.; Zygourakis, K.; Barnes, R.T. Hydrologic properties of biochars produced at different temperatures. *Biomass Bioenergy* **2012**, *41*, 34–43.
36. Liu, Z.; Dugan, B.; Masiello, C.A.; Gonnermann, H.M. Biochar particle size, shape, and porosity act together to influence soil water properties. *PLoS ONE* **2017**, *12*, e0179079.
37. Pituello, C.; Dal Ferro, N.; Francioso, O.; Simonetti, G.; Berti, A.; Piccoli, I.; Pisi, A.; Morari, F. Effects of biochar on the dynamics of aggregate stability in clay and sandy loam soils. *Eur. J. Soil Sci.* **2018**, *69*, 827–842, doi:10.1111/ejss.12676.
38. Kumari, K.G.I.D.; Moldrup, P.; Paradelo, M.; Elsgaard, L.; de Jonge, L.W. Effect of Biochar on Dispersibility of Colloids in Agricultural Soils. *J. Environ. Qual.* **2017**, *46*, 143–152.
39. Ghorbani, M.; Asadi, H.; Abrishamkesh, S. Effects of rice husk biochar on selected soil properties and nitrate leaching in loamy sand and clay soil. *Int. Soil Water Conserv. Res.* **2019**, *7*, 258–265.
40. Major, J.; Rondon, M.; Molina, D.; Riha, S.J.; Lehmann, J. Nutrient leaching in a Colombian savanna oxisol amended with biochar. *J. Environ. Qual.* **2012**, *41*, 1076–1086.
41. Hardie, M.; Clothier, B.; Bound, S.; Oliver, G.; Close, D. Does biochar influence soil physical properties and soil water availability? *Plant Soil* **2014**, *376*, 347–361.
42. Jeffery, S.; Meinders, M.B.J.; Stoof, C.R.; Bezemer, T.M. van de Voorde, T.F.J.; Mommer, L. van Groenigen, J.W. Biochar application does not improve the soil hydrological function of a sandy soil. *Geoderma* **2015**, *251–252*, 47–54.
43. Castellini, M.; Giglio, L.; Niedda, M.; Palumbo, A.D.; Ventrella, D. Impact of biochar addition on the physical and hydraulic properties of a clay soil. *Soil Tillage Res.* **2015**, *154*, 1–13.
44. Soil Survey Staff. Soil taxonomy: A basic system of soil classification for making and interpreting soil surveys, 2nd ed. In *Natural Resources Conservation Service. Handbook 436*; United States Department of Agriculture: Washington, DC, USA, 1999.
45. Bremner, J.M. Nitrogen-total. In *Methods of Soil Analysis Part 3—Chemical Methods*; SSSA Book Ser. No. 5; Sparks, D.L., Page, A.L., Johnston, C.T., Summ, M.E., Eds.; SSSA: Madison, WI, USA, 1996; pp. 1058–1121.
46. Olsen, S.R.; Cole, C.V.; Watanabe, F.S.; Dean, L.A. *Estimation of Available Phosphorus in Soil by Extraction with Sodium Bicarbonate*; USDA Circular 939; USDA: Washington, DC, USA, 1954; pp. 1–19.
47. Walkley, A.; Black, I.A. An examination of the Degtjareff method for determining soil organic matter and a proposed modification of the chromic acid titration method. *Soil Sci.* **1934**, *37*, 29–38.
48. Chan, K.Y.; Xu, K. Biochar: Nutrient properties and their enhancement. In *Biochar for Environmental Management. Science and Technology*; Lehmann, J., Joseph, S., Eds.; Earthscan: London, UK, 2009; pp. 67–84.
49. EBC. *European Biochar Certificate Guidelines for a Sustainable Production of Biochar*; European Biochar Certificate (EBC): Arbaz, Switzerland, 2012.

50. IBI. *International Biochar Initiative, Standardized Product Definition and Product Testing Guidelines for Biochar That Is Used in Soil*; IBI-STD-2.0; IBI: Toronto, ON, Canada, 2014.
51. Klute, A.; Dirksen, C. Hydraulic conductivity and diffusivity: Laboratory methods. In *Methods of Soil Analysis-Part 1. Physical and Mineralogical Methods*; Klute, A., Ed.; Wiley: Hoboken, NJ, USA, 1986; pp. 687–734.
52. Reynolds, W.D.; Drury, C.F.; Tan, C.S.; Fox, C.A.; Yang, X.M. Use of indicators and pore volume-function characteristics to quantify soil physical quality. *Geoderma* **2009**, *152*, 252–263.
53. Walters, R.D.; White, J.G. Biochar In Situ Decreased Bulk Density and Improved Soil-Water Relations and Indicators in South-eastern US Coastal Plain Ultisols. *Soil Sci.* **2018**, *183*, 99–111.
54. van Genuchten, M. Th. A closed form equation for predicting the hydraulic conductivity of unsaturated soils. *Soil Sci. Soc. Am. J.* **1980**, *44*, 892–898.
55. Mualem, Y. A new model for predicting the hydraulic conductivity of unsaturated porous media. *Water Resour. Res.* **1976**, *12*, 513–522.
56. METER Group. *Mini Disk Infiltrometer-User's Manual*. Decagon Devices, Inc.: Pullman, WA, USA, 2014; pp. 10-14.
57. Zhang, R. Infiltration models for the disk infiltrometer. *Soil Sci. Soc. Am. J.* **1997**, *61*, 1597–1603.
58. Philip, J.R. The theory of infiltration: 4. Sorptivity and algebraic infiltration equations. *Soil Sci.* **1957**, *84*, 257–264.
59. Edeh, I.G.; Mašek, O.; Buss, W. A meta-analysis on biochar's effects on soil water properties—New insights and future research challenges. *Sci. Total Environ.* **2020**, *714*, 136857, doi:10.1016/j.scitotenv.2020.136857.
60. Kayode, S.A. 2019 Biochar and Soil Physical Health. In *Biochar—An Imperative Amendment for Soil and the Environment*; Vikas, A., Peeyush, S., Eds.; IntechOpen: London, UK, 2019, doi:10.5772/intechopen.83706. Available online: <https://www.intechopen.com/books/biochar-an-imperative-amendment-for-soil-and-the-environment/biochar-and-soil-physical-health> (accessed on 20 December 2020).
61. Quin, P.R.R.; Cowie, A.L.; Flavel, R.J.; Keen, B.P.; Macdonald, L.M.; Morris, S.G.; Singh, B.P.; Young, I.M.; Zwieten, L. Oil mallee biochar improves soil structural properties—A study with x-ray micro-CT. *Agric. Ecosyst. Environ.* **2014**, *191*, 142–149, doi:10.1016/j.agee.2014.03.022.
62. Zhao, S.X.; Ta, N.; Wang, X.D. Effect of temperature on the structural and physico-chemical properties of biochar with apple tree branches as feedstock material. *Energies* **2017**, *10*, doi:10.3390/en10091293.
63. Hyväluoma, J.; Kulju, S.; Hannula, M.; Wikberg, H.; Källi, A.; Rasa, K. Quantitative characterization of pore structure of several biochars with 3D imaging. *Environ. Sci. Pollut. Res.* **2018**, *25*, 25648–25658, doi:10.1007/s11356-017-8823-x.
64. Ouyang, L.; Wang, F.; Tang, J.; Yu, L.; Zhang, R. Effects of biochar amendment on soil aggregates and hydraulic properties. *J. Soil Sci. Plant Nutr.* **2013**, *13*, 991–1002.
65. Aller, D.; Rathke, S.; Laird, D.; Crusea, R.; Hatfield, J. Impacts of fresh and aged biochars on plant available water and water use efficiency. *Geoderma* **2017**, *307*, 114–121.
66. Mia, S.; Dijkstra, F.A.; Singh, B. Long-term aging of biochar: A molecular understanding with agricultural and environmental implications. *Adv. Agron.* **2017**, *141*, 1–51.
67. Günala, E.; Erdem, H.; Çelik, İ. Effects of three different biochars amendment on water retention of silty loam and loamy soils. *Agric. Water Manag.* **2018**, *208*, 232–244.